Van der Waals Heteroepitaxial AZO/NiO/AZO/Muscovite (ANA/muscovite) Transparent Flexible Memristor

Van der Waals Heteroepitaxial AZO/NiO/AZO/Muscovite (ANA/muscovite) Transparent Flexible Memristor

Van-Qui Le, Thi-Hien Do, José Ramón Durán Retamal, Pao-Wen Shao, Yu-Hong Lai, Wen-Wei Wu, Jr-Hau He, Yu-Lun Chueh, Ying-Hao Chu

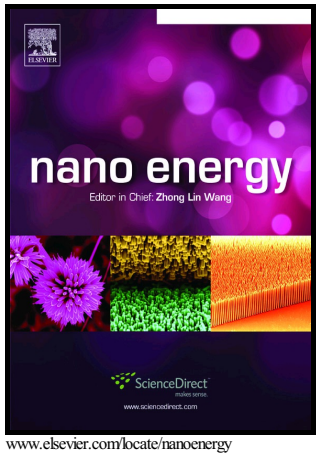

www.elsevier.com/locate/nanoenergy

PII: S2211-2855(18)30770-5
DOI: https://doi.org/10.1016/j.nanoen.2018.10.042
Reference: NANOEN3120

To appear in: *Nano Energy*

Received date: 31 August 2018
Revised date: 13 October 2018
Accepted date: 20 October 2018

Cite this article as: Van-Qui Le, Thi-Hien Do, José Ramón Durán Retamal, Pao-Wen Shao, Yu-Hong Lai, Wen-Wei Wu, Jr-Hau He, Yu-Lun Chueh and Ying-Hao Chu, Van der Waals Heteroepitaxial AZO/NiO/AZO/Muscovite (ANA/muscovite) Transparent Flexible Memristor, *Nano Energy,* https://doi.org/10.1016/j.nanoen.2018.10.042

van der Waals Heteroepitaxial AZO/NiO/AZO/Muscovite (ANA/muscovite) Transparent Flexible Memristor

Van-Qui Le[a], Thi-Hien Do[a], José Ramón Durán Retamal[c], Pao-Wen Shao[a], Yu-Hong Lai[a], Wen-Wei Wu[a,h], Jr-Hau He[c], Yu-Lun Chueh*[b, f, g] and Ying-Hao Chu*[a,d,e]

[a]Department of Materials Science and Engineering, National Chiao Tung University, Hsinchu 30010, Taiwan

[b]Department of Materials Science and Engineering, National Tsing Hua University, Hsinchu 30013, Taiwan

[c]Computer, Electrical and Mathematical Science and Engineering, King Abdullah University of Science & Technology, Thuwal 23955-6900, Kingdom of Saudi Arabia.

[d]Material and Chemical Research Laboratories, Industrial Technology Research Institute, 31040, Taiwan.

[e]Center for Emergent Functional Matter Science, National Chiao Tung University, Hsinchu 30010, Taiwan.

[f]Frontier Research Center on Fundamental and Applied Sciences of Matters, National Tsing Hua University, Hsinchu 30013, Taiwan.

[g]Department of Physics, National Sun Yet-Sun University, Kaohsiung, 80424, Taiwan, Republic of China

[h]Center for the Intelligent Semiconductor Nano-system Technology Research, National Chiao Tung University, Hsinchu 300, Taiwan

ylchueh@mx.nthu.edu.tw

yhchu@g2.nctu.edu.tw

ABSTRACT-

Multifunctional electronics featuring optical transparency, portability, mechanical flexibility, light-weight and environment-friendly are of great demands for next-generation smart electronics. Memristor represents one of the important chains in next-generation devices as the information computing and storage component. Here, we design the transparent flexible structure based on van der Waals heteroepitaxial AZO/NiO/AZO/muscovite (ANA/muscovite) for a memristor application. The (ANA/muscovite) memristor satisfies all the hardest requirements of a transparent soft device such as optical transparency over 80 % in visible light and high performance with a ON/OFF resistance ratio $>10^5$, stable endurance to 10^3 cycles and long retention time of 10^5 s**.** In addition, the ANA/muscovite memristor can work at various bending radii down to 5 mm, a mechanical bending after 1000 cycles at a curvature with a radius of 6.5 mm and a high temperature up to 185 ^oC, which deliver a pathway for future applications in flexible transparent smart electronics.

Graphical Abstract:

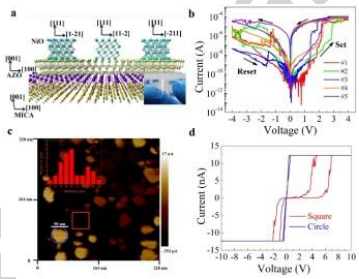

Keywords:

AZO/NiO/AZO/muscovite, aluminum doped zinc oxide (AZO), van der Waals, transparent flexible memristor

1. Introduction

The advantages of the Internet of Thing (IoT) generator greatly change our daily life, creating a strong demand on smart electronics with multifunctionalities such as mechanical flexibility, light-weight, stretchability, wearability, optical transparency, environmental friendliness and robustness to satisfy the requirements of the IoT generator. Thus, it has attracted significant attention from both academic and industrial communities[1],[2]. Along with this research direction, transparent flexible devices, including transistors[3–7], photodetectors[8,9], displays[10–12], sensors[13–15], triboelectric nanogenerator[16,17] and nonvolatile memory devices[18],[19,20] have played a critical role in various types of smart electronic applications. Among them, memristors or resistive switching memories[21–23] can store and process information by recording changes of resistance states under an external electric field. Therefore, they have been widely investigated as one of the most promising candidates for next-generation logical, computing, synaptic, and nonvolatile memory devices due to its simple structures, small size, high speed, low power consumption, good endurance, long retention and cost-effective[21,24–27]. In previous studies, transparent flexible memristors have been successfully fabricated on polymer substrates e.g. soft polydimethylsiloxane[19], colorless polyimide[20], polyethylene terephthalate[28],[29] and polyethersulfone[30]. These substrates show the good mechanical flexibility compared to conventional substrates. However, there are critical features of polymer materials such as low processing temperature and poor adhesion. Thus, these devices typically result in the poor crystallinity and the short lifetime without the good thermal stability. Recently, muscovite mica is considered as a good template to epitaxially integrate functional materials for flexible and transparent electronics due to its unique characteristics[31,32]. Firstly, the atomically smooth surface and the high melting point (1150–1300 K) make the muscovite compatible with the fabrication processes of most functional materials. Secondly, the thickness of the muscovite can be reduced to few microns by the exfoliation technique due to the weak van der Waals interaction

between interlayers of the muscovite, which creates unconstrained films with the superior mechanical flexibility. Thirdly, the muscovite displays the high optical transparency associated with the chemical inertness, making it suitable in the applications of environmental robustness. Therefore, a new platform called MICAtronics[31,32] has been created to build up oxide heteroepitaxy for novel transparent soft technology with superior chemical and thermal stabilities.

In this work, a transparent flexible memristor based on the van der Waals heteroepitaxial growth composed of Al-doped ZnO (AZO)/NiO/AZO (ANA) sandwich structure on the muscovite substrate was fabricated. NiO is a promising candidate for transparent flexible memristor applications, which is attributed to its wide band gap (3.6-4.0 eV), high-temperature stability and reliable memory characteristics[33–37],[38,39]. In addition, AZO is suggested as a possible solution for the next-generation transparent conducting electrode[40]. Interestingly, ANA/muscovite memristor exhibits not only transparent and flexible memristor with the ON/OFF resistance ratio $>10^5$, the stable endurance to 10^3 cycles and the long retention time of 10^5 s, but also the excellent electrical performances together with the mechanical flexibility, the durability and the thermal stability**.** In addition, the ANA/muscovite memristor can work at various bending radii down to 5 mm, the mechanical bending after 1000 cycles at the bending radius of 6.5 mm and the high temperature up to 185 ^{o}C, which deliver a pathway for future applications in flexible transparent smart electronics. This study marks an important milestone in the advancement of transparent flexible nonvolatile electronics for next-generation smart wearable devices.

2. Material and methods

Sample preparation. Commercial AZO (2 %Al) and NiO targets were used to deposit AZO and NiO layers on a (001) muscovite substrate by the pulsed laser deposition method. A KrF excimer laser (λ = 248nm) was operated at a repetition rate of 10 Hz with the laser energy of 1 J/cm^{-2}. The first, 120 nm AZO film were grown on mica as a bottom electrode with a

substrate temperature of 420 °C in 0.1 mTorr oxygen pressure. Then, NiO thin film were deposited on AZO/mica at a substrate temperature from 400-600 °C in high vacuum from 0.01-10 mTorr in oxygen environment to optimize the conditions. The best performance of device is 120 nm NiO/ (120 nm) AZO/muscovite mica at temperature and pressure 0.1 mT.

Structural Characterizations.

A Bruker D8 X-ray diffractometer equipped Cu $K\alpha_1$ radiation (λ=1.5406A^0) was employed to obtain structural information. The details of the microstructure were investigated by using spherical-aberration corrected transmission electron microscope (Cs-TEM, JEOL ARM 200F) at room temperature kV. The samples were prepared by a focused ion beam (FIB) in a cross-sectional geometry. Conductive atomic force microscopy was measured by using Innova (Bruker) microscope. The optical spectra were collected in the transmission mode using a Perkin-Elmer Lambda-900 spectrometer (200－2600 nm).

I-V measurements.

The electrical characterizations and resistive switching characteristics of the fabricated devices were investigated using a Keithley 4200 semiconductor parameter analyzer in voltage sweeping mode. All of the operation voltages were applied on the top AZO electrode, and the AZO bottom electrode was grounded. The current compliance of 100 μA was applied to avoid the breakdown of the memristor device. A home-made bending stage was used to set up different radii. The temperature change measurement system was used to measure resistance with the temperature ranging from 25 ^oC to 185 ^oC.

3. Results and Discussion

The NiO film was directly fabricated on a 50 μm-thick muscovite substrate with the AZO layer as the bottom electrode via the pulsed laser deposited (PLD) method. The details on the growth

conditions can be found in the method session. A shadow mask with the circle shape of 200 μm in diameter was used to define the diameter of top AZO electrodes. The natural photographs and its schematic of ANA/muscovite heterostructure are shown in Fig. 1(a) and the inset. The logo at the bottom can be easily observed through the structure due to the high optical transparency of AZO, NiO and muscovite layers as shown in the inset of Fig. 1(b), of which the corresponding transmittance behaviors were measured as shown in Fig. 1(b). Clearly, the optical transmittance of the ANA/muscovite structure is over 80 % at the wavelength higher than 550 nm in the visible wavelength region between 300 to 800 nm. Furthermore, the phases and crystal structures of the heterostructure were investigated by X-ray diffraction (XRD). Fig. 1(c) shows XRD 2θ-θ scans of ANA/muscovite heterostructure. Only muscovite (*00l*), AZO (*00l*) and NiO (*lll*) diffraction peaks were detected, indicating the epitaxial feature of the heterostructure without any impurity phase. The estimated out-of-plane lattice constants of NiO (0.42 nm) and AZO (0.5218 nm) suggest the small compressive strains of 0.33 % and 0.17 %, respectively. This feature is similar to some earlier research about the grown epitaxial materials on muscovite substrates,[40–44]. In addition, the in-plane structural relationships are obtained by analyzing the ϕ-scan results of NiO {022}, AZO {101} and muscovite {202} diffraction peaks as shown in Fig. 1(d). The six-fold symmetry of AZO {101} indicates that a single-crystalline AZO layer is epitaxially grown on the muscovite substrate. Meanwhile, the six symmetric peaks of the NiO {022} suggest that the NiO possesses three sets of structural domains. The epitaxial relationship can be determined as NiO(111)//AZO(001)//muscovite(001) and NiO[01-1]//AZO[010]//muscovite[010]. In order to examine the interface structure, the heterostructure was further investigated by transmission electron microscopy (TEM) as shown in Fig. 1(e). The cross-sectional TEM image reveals the layer structure of the ANA/muscovite heterostructure (left panel in Fig. 1(e)). The high-resolution TEM images exhibit defect-free and coherent interfaces at the interfaces of NiO/AZO and AZO/muscovite in the heterostructure (middle panel in Fig. 1(e)). The Fast Fourier Transform (FFT)

patterns of interlayers (right panel in Fig. 1(e)) (NiO (blue and orange), AZO (red) and muscovite (yellow)) in the insets show the epitaxial relationship as NiO[111]//AZO[001]//muscovite[001] and NiO[01-1]//AZO[010]//muscovite[010], which are consistent with the XRD results. A schematic of the NiO/AZO heterostructure grown on muscovite with the orientation relationship is constructed and shown in Fig. 1(f). These results demonstrate high-quality transparent ANA/muscovite heteroepitaxy was fabricated.

To investigate the device performance of memristor based on the ANA/muscovite heteroepitaxy, the bottom electrode was grounded and a voltage was swept to the top electrode. An exploration of the optimized electrical performance was carried out by tuning growth conditions and varying the thicknesses of NiO layers. The ratio of resistance change in various conditions can be found in (Fig. S1, Supporting Information). In Fig. 2(a), the I-V curve operated with a sequence of 0-+4V-0--4V-0 on five different memristors show the same shape in the operation of a positive bias. The set process is defined as the change of resistance from high resistance state (HRS) to low resistance state (LRS). On the contrary, the resistance changed from LRS to HRS is called the reset process. Interestingly, these memristors exhibit a typical bipolar resistive switching with a high ratio of resistance change $>10^5$ without the electroforming process, namely forming free. Note that the voltages are read at 0.5 V as V_{SET} and V_{RESET} and the resistance of HRS and LRS at V_{SET} and V_{RESET} are defined as R_{HRS} and R_{LRS}, respectively. Even though the I-V curves in the negative bias process are unstable, they are necessary for the repeating in the positive bias process. In Fig. 2(b), the performances of electrical endurance and retention of the fifth device are shown in the set process at the bias of 0.5 V. The device can be operated repeatable up to over 1000 cycles without the obvious degradation after 10^5 s, delivering excellent electrical endurance. The cumulative statistical probability of the device shows a uniform distribution of HRS and LRS (Fig. S2 in the Supporting Information). These characteristics confirmed that the ANA/mica heteroepitaxy is applicable to a highly transparent memristor device.

To understand the conduction mechanism of the ANA/muscovite memristor during resistive switching, the models of the Ohmic and space-charge-limited conduction (SCLC) (Fig. 3(a)) and conductive atomic force microscopy (c-AFM) have been examined. The fitting results of the logI-logV plots in Fig. 3(b) suggest that the conduction mechanism in the HRS region is the SCLC while the Ohmic conduction mechanism dominates in the LRS region. Moreover, the surface of NiO layer was examined by the current mapping of c-AFM (Fig. 3(c)) where many conductive spots (circle region) with diameters from 10 nm to 100 nm (inset in Fig. 3(c)) distributed on the surface were confirmed. The conductive spots display a higher density in LRS as compared to HRS. In addition, these conductive spots show different I-V characteristics in Fig. 3(d). At the square region, I-V curves present a typical bipolar memristive behavior while it expresses a linear I-V characteristic at the circle region (90 nm in diameter). The results of c-AFM directly exhibit an evidence of the formation and removal of filaments on the surface, which supports the filament model as the switching mechanism in the memristor. Based on the above experimental results (Fig. 3(a)) and theoretical analysis (Fig. 3(b)), a schematic diagram of the switching mechanism is illustrated in Fig. 3(e) and Fig. 3(f). In fact, the growth of AZO and NiO layers was executed in a relatively low oxygen environment, thus the existence of oxygen vacancies is highly expected. In the set process, the accumulation of oxygen vacancies to form the conduction channel is driven by the external electrical field while the conduction path is broken in the reset process, resulting in the resistance change between HRS and LRS. To shed light on the oxygen-vacancy driven conduction, the investigation of TEM was conducted. However, due to the dark contrast of the NiO crystalline layer, it is difficult to look for the existence of filaments with obvious contrast. In addition, no other phases were found after the devices were switched to LRS under the TEM study, implying the proposed model based on the motion of oxygen vacancies is the dominated one.

To address the thermal stability of memristor devices, electrical characteristics of transparent flexible ANA/muscovite memristors were measured at different temperatures ranging from 25 ^{o}C

(room temperature) to 185 ^{o}C with an incremental step of 15 ^{o}C as shown in Fig. 4(a). To shed light on the performance of the devices, the complete device characteristics at selected temperatures at 25, 85, 125 and 185 ^{o}C are shown in (Fig. S3 of the Supporting Information), revealing the properties of the threshold resistive switching. The linear fitted of Vthreshold and Vhold was analyzed from I-V curves as a function of voltage versus temperature (Fig. 4(c)). Furthermore, the I-V curves exhibited a high resistance ratio with the R_{HRS}/R_{LRS} of ~10^5 at 25 ^{o}C and decrease to ~10^3 at 185 ^{o}C (Fig. 4(d)) . The thermal activation energy (E_a), which represents the location of defect levels below the conduction band, can be calculated by an Arrhenius plot using the relationship $I = I_o\exp(E_a/kT)$ where k is the Boltzmann constant and T is the absolute temperature. The thermal activation energy of HRS and LRS can be extracted to be 0.66 and 0.15 eV, respectively as shown in Fig. 4(b). The difference of the activation energy conforms to the difference in the carrier conduction mechanisms between HRS and LRS**.** In addition, the I-V tests on electrical endurance, and retention were carried out (Fig. S4, 5, Supporting Information) show that the high ratio of resistance maintained at different temperature increase from 25 ^{o}C to 185 ^{o}C. Note that the ON/OFF ratio higher than 10^3 remains at 185 ^{o}C, demonstrating the good memory reliability at an elevated temperature. These results suggest that the ANA/muscovite memristor device can safely work in the temperature ranges of 25-185 ^{o}C.

To verify the mechanical flexibility of the ANA/muscovite memristor, the I-V test under three kinds of strain including flat, tensile (inset in Fig. 5(a)) and compressive (inset in Fig. 5(d)) modes were examined. (Fig. S6, Supporting Information) were examined. I-V behaviors under different tensile and compressive bending curves were investigated (Fig. S7(a), Supporting Information). There is no obvious change of the I-V characteristics under various bending conditions. The ratios of R_{HLS}/R_{LRS} as the function of bending radii at 0.5 V were extracted as shown in Fig. 5(a). A slight degradation of the R_{HRS}/R_{LRS} ratio happens when radius is smaller than 8 mm in the positive bias region, but overall, there is negligible change in electrical performance upon the bending.

Furthermore, endurance and retention characteristics of the ANA/muscovite memristor were tested under tensile and compressive bending tests with the bending radii ranging from 15 to 5 mm as shown in Fig. 5(b) and Fig. 5(c). The I-V behaviors of memristor were maintained with the ratio of 10^5 in 1000 cycles and longer than 10^4 s while the only slight degradation can be observed at 5 mm of radius. To investigate the mechanical reliability, the memristor was bent continuously up to 1000 cycles at the bending radius of 6.5 mm. The I-V curves (Fig. S7(b), Supporting Information) and the R_{HRS}/R_{LRS} ratios are shown in Figure 5d, indicating no clear degradation. In addition, the endurance and retention under the mechanical bending at the bending radius of 6.5 mm were also carried out as shown in Fig. 5(e) and Fig.5(f). The memory device shows the good endurance performance up to 300 cycles without the significant variation in current states. A comparison of the memristors composed of the NiO layer on rigid substrates, muscovite and other transparent flexible memristors is summarized in Table 1. Clearly, the AZO/NiO/AZO/muscovite (ANA/muscovite) memristor satisfies all the hardest requirements of a transparent soft device such as optical transparency over 80 % in visible light, high performance with a ON/OFF resistance ratio $>10^5$, stable endurance to 10^3 cycles and long retention time (10^5 s)**.** In addition, the AZO/NiO/AZO/muscovite memristor can work under various bending radii down to 5 mm, mechanical bending after 1000 cycles at the bending radius of 6.5 mm and high temperature up to 185 ^oC, which deliver a pathway for future applications in flexible transparent smart electronics.

4. Conclusions

A transparent flexible memristor based on the NiO/AZO/muscovite heteroepitaxy with aluminum doped zinc oxide (AZO) electrodes was demonstrated. The ANA/muscovite heteroepitaxy exhibits of transparent flexible memristor behaviors with the high performance ($R_{HRS}/R_{LRS} \sim 10^5$) repeating in 1000 cycles and the long retention time (10^5 s). The reliable mechanical flexibility of memristor device was shown at various bending radii (R_{min} = 5 mm) and over 1000 bending cycles at the bending radius of 6.5 mm. Interestingly, it can also be worked at

high-temperature environment up to 185 °C. Such results deliver a new heterostructure based on oxide heteroepitaxy for the soft transparent memristor.

Acknowledgments

This work is supported by the Ministry of Science and Technology, Taiwan (Grant Nos. MOST 106-2119-M-009-011-MY3, 106-2628-E-009-001-MY2, 106-2923-M-009-003-MY2, 105-2633-M-007-003, 106-2112-M-007-028-MY3, 107-2923-E-007-002 -MY3, 107-2112-M-007-030-MY3, 06-2923-E-007-006-MY2, 105-2119-M-009-009, 107-3017-F-007-002 and the Center for Emergent Functional Matter Science of National Chiao Tung University from The Featured Areas Research Center Program within the framework of the Higher Education Sprout Project by the Ministry of Education (MOE) in Taiwan. The author W.W.W. acknowledges the support from Ministry of Science and Technology (MOST) in Taiwan (MOST-107-3017-F-009-002) and "Center for the Intelligent Semiconductor Nano-system Technology Research, National Chiao Tung University" from The Featured Areas Research Center Program within the framework of the Higher Education Sprout Project by the Ministry of Education (MOE) in Taiwan.

Appendix A. Supporting Information

I-V characteristics as functions of the growth conditions; The cumulative statistical probability of the device; I -V characteristics within a variety of temperatures; Endurance and retention results at different temperatures; I-V characteristics without and within the tensile bending and the compressive bending and I-V characteristics with the tensile bending and the compressive bending at 6.5 mm of the radius; This material is available for free of charge.

References

[1] S.R. Forrest, The path to ubiquitous and low-cost organic electronic appliances on plastic, Nature. 428 (2004) 911–918.

[2] M.T. Ghoneim, M.M. Hussain, M. Jacob, Review on physically flexible nonvolatile memory for internet of everything electronics, Electronics. 4 (2015) 424–479.

[3] K. Nomura, H. Ohta, A. Takagi, T. Kamiya, M. Hirano, H. Hosono, Room-temperature fabrication of transparent flexible thin-film transistors using amorphous oxide semiconductors, Nature. 432 (2004) 488–492.

[4] G. Eda, G. Fanchini, M. Chhowalla, Large-area ultrathin films of reduced graphene oxide as a transparent and flexible electronic material, Nat. Nanotechnol. 3 (2008) 270–274.

[5] T. Georgiou, R. Jalil, B.D. Belle, L. Britnell, R. V Gorbachev, S. V Morozov, Y.-J. Kim, A. Gholinia, S.J. Haigh, O. Makarovsky, L. Eaves, L.A. Ponomarenko, A.K. Geim, K.S. Novoselov, A. Mishchenko, Vertical field-effect transistor based on graphene-WS_2 heterostructures for flexible and transparent electronics, Nat. Nanotechnol. 8 (2012) 100–103.

[6] S. Ju, A. Facchetti, Y. Xuan, J. Liu, F. Ishikawa, P. Ye, C. Zhou, T.J. Marks, D.B. Janes, Fabrication of fully transparent nanowire transistors for transparent and flexible electronics, Nat. Nanotechnol. 2 (2007) 378–384.

[7] H. Zhu, L. Hu, J. Cumings, J. Huang, Y. Chen, Highly Transparent and Flexible Nanopaper Transistor., ACS Nano. (2013) 2106–2113.

[8] Z.Q. Zheng, J.D. Yao, G.W. Yang, Growth of centimeter-scale high-quality In_2Se_3 films for transparent, flexible and high performance photodetectors, J. Mater. Chem. C. 4 (2016) 8094–8103.

[9] Z. Zheng, L. Gan, H. Li, Y. Ma, Y. Bando, D. Golberg, T. Zhai, A fully transparent and flexible ultraviolet-visible photodetector based on controlled electrospun ZnO-CdO heterojunction nanofiber arrays, Adv. Funct. Mater. 25 (2015) 5885–5894.

[10] L. Zhou, H.-Y. Xiang, S. Shen, Y.-Q. Li, J.-D. Chen, H.-J. Xie, I.A. Goldthorpe, L.-S. Chen, S.-T. Lee, J.-X. Tang, High-performance flexible organic light-emitting diodes using embedded silver network transparent electrodes, ACS Nano. 8 (2014) 12796–12805.

[11] N. Guan, X. Dai, A. Messanvi, H. Zhang, J. Yan, E. Gautier, C. Bougerol, F.H. Julien, C. Durand, J. Eymery, M. Tchernycheva, Flexible white light emitting diodes based on nitride

nanowires and nanophosphors, ACS Photonics. 3 (2016) 597–603.

[12] D. Zhang, K. Ryu, X. Liu, E. Polikarpov, J. Ly, M.E. Tompson, C. Zhou, Transparent, conductive, and flexible carbon nanotube films and their application in organic light-emitting diodes, Nano Lett. 6 (2006) 1880–1886.

[13] Q. Wang, M. Jian, C. Wang, Y. Zhang, Carbonized Silk Nanofiber Membrane for Transparent and Sensitive Electronic Skin, Adv. Funct. Mater. 27 (2017) 1–9.

[14] M.S. Sarwar, Y. Dobashi, C. Preston, J.K.M. Wyss, S. Mirabbasi, J.D.W. Madden, Bend, stretch, and touch: Locating a finger on an actively deformed transparent sensor array, Sci. Adv. 3 (2017) e1602200.

[15] M. Segev-bar, H. Haick, Flexible sensors based on nanoparticles, ACS Nano. 7 (2013) 8366–8378.

[16] B.N. Chandrashekar, B. Deng, A.S. Smitha, Y. Chen, C. Tan, H. Zhang, H. Peng, Z. Liu, Roll-to-Roll green transfer of CVD graphene onto plastic for a transparent and flexible triboelectric nanogenerator, Adv. Mater. 27 (2015) 5210–5216.

[17] J. Wang, Z. Wen, Y. Zi, P. Zhou, J. Lin, H. Guo, Y. Xu, Z.L. Wang, All plastic materials based self charging power system composed of triboelectric nanogenerators and supercapacitors, Adv. Funct. Mater. 26 (2016) 1070–1076.

[18] K.L. Kim, W. Lee, S.K. Hwang, S.H. Joo, S.M. Cho, G. Song, S.H. Cho, B. Jeong, I. Hwang, J.H. Ahn, Y.J. Yu, T.J. Shin, S.K. Kwak, S.J. Kang, C. Park, Epitaxial growth of thin ferroelectric polymer films on graphene layer for fully transparent and flexible nonvolatile memory, Nano Lett. 16 (2016) 334–340.

[19] K. Qian, R.Y. Tay, M.F. Lin, J. Chen, H. Li, J. Lin, J. Wang, G. Cai, V.C. Nguyen, E.H.T. Teo, T. Chen, P.S. Lee, Direct observation of indium conductive filaments in transparent, flexible, and transferable resistive switching memory, ACS Nano. 11 (2017) 1712–1718.

[20] S.-W. Yeom, B. You, K. Cho, H.Y. Jung, J. Park, C. Shin, B.-K. Ju, J.-W. Kim, Silver

nanowire/colorless-polyimide composite electrode: Application in flexible and transparent resistive switching memory, Sci. Rep. 7 (2017) 3438.

[21] D.B. Strukov, G.S. Snider, D.R. Stewart, R.S. Williams, The missing memristor found, Nature. 453 (2008) 80–83.

[22] L. Chua, Resistance switching memories are memristors, Appl. Phys. A Mater. Sci. Process. 102 (2011) 765–783.

[23] Y. Yang, W. Lu, Nanoscale resistive switching devices: mechanisms and modeling, Nanoscale. 5 (2013) 10076.

[24] J.J. Yang, D.B. Strukov, D.R. Stewart, Memristive devices for computing, Nat. Nanotechnol. 8 (2013) 13–24.

[25] Z. Wang, S. Joshi, S.E. Savel'ev, H. Jiang, R. Midya, P. Lin, M. Hu, N. Ge, J.P. Strachan, Z. Li, Q. Wu, M. Barnell, G.-L. Li, H.L. Xin, R.S. Williams, Q. Xia, J.J. Yang, Memristors with diffusive dynamics as synaptic emulators for neuromorphic computing, Nat. Mater. 16 (2016) 101–108.

[26] H.-S.P. Wong, S. Salahuddin, Memory leads the way to better computing, Nat. Nanotechnol. 10 (2015) 191–194.

[27] M.K. Hota, M.N. Hedhili, N. Wehbe, M.A. McLachlan, H.N. Alshareef, Multistate resistive switching memory for synaptic memory applications, Adv. Mater. Interfaces. 3 (2016).

[28] M. Kim, K.C. Choi, Transparent and flexible resistive random access memory based on Al_2O_3 film with multilayer electrodes, IEEE Trans. Electron Devices. 64 (2017) 3508–3510.

[29] K.N. Pham, V.D. Hoang, C.V. Tran, TiO_2 thin film based transparent flexible resistive switching random access memory, Adv. Nat. Sci. Nanosci. 7 (2016) 015017.

[30] J. Won Seo, J.W. Park, K.S. Lim, S.J. Kang, Y.H. Hong, J.H. Yang, L. Fang, G.Y. Sung, H.K. Kim, Transparent flexible resistive random access memory fabricated at room temperature, Appl. Phys. Lett. 95 (2009) 1–4.

[31] Y.-H. Chu, Van der Waals oxide heteroepitaxy, Npj Quantum Mater. 2 (2017) 67.

[32] Y. Bitla, Y.H. Chu, MICAtronics: A new platform for flexible X-tronics, FlatChem. 3 (2017) 26–42.

[33] J.Y. Son, Y.H. Shin, Direct observation of conducting filaments on resistive switching of NiO thin films, Appl. Phys. Lett. 92 (2008) 2006–2009.

[34] J.G. Park, W.S. Nam, S.H. Seo, Y.G. Kim, Y.H. Oh, G.S. Lee, U.G. Paik, Multilevel nonvolatile small-molecule memory cell embedded with Ni nanocrystals surrounded by a NiO tunneling barrier, Nano Lett. 9 (2009) 1713–1719.

[35] K.M. Kim, S.J. Song, G.H. Kim, J.Y. Seok, M.H. Lee, J.H. Yoon, J. Park, C.S. Hwang, Collective motion of conducting filaments in Pt/n-type TiO_2/p-type NiO/Pt stacked resistance switching memory, Adv. Funct. Mater. 21 (2011) 1587–1592.

[36] B.K. You, W.I. Park, J.M. Kim, K. Il Park, H.K. Seo, J.Y. Lee, Y.S. Jung, K.J. Lee, Reliable control of filament formation in resistive memories by self-assembled nanoinsulators derived from a block copolymer, ACS Nano. 8 (2014) 9492–9502.

[37] A. Liu, H. Zhu, Z. Guo, Y. Meng, G. Liu, E. Fortunato, R. Martins, F. Shan, Solution combustion synthesis: low-temperature processing for p-type Cu:NiO thin films for transparent electronics, Adv. Mater. (2017). DOI 10.1002/adma.201701599.

[38] M.Q. Guo, Y.C. Chen, C.Y. Lin, Y.F. Chang, B. Fowler, Q.Q. Li, J. Lee, Y.G. Zhao, Unidirectional threshold resistive switching in Au/NiO/Nb:$SrTiO_3$ devices unidirectional threshold resistive switching in Au/NiO/Nb:$SrTiO_3$ devices, Appl. Phys. Lett. 110 (2017) 233504.

[39] Z. Sun, Y. Zhao, M. He, L. Gu, C. Ma, K. Jin, D. Zhao, N. Luo, Q. Zhang, N. Wang, W. Duan, C. Nan, Deterministic role of concentration surplus of cation vacancy over anion vacancy in bipolar memristive NiO, ACS Appl. Mater. Interfaces. 8 (2016) 11583–11591.

[40] Y. Bitla, C. Chen, H.C. Lee, T.H. Do, C.H. Ma, L. Van Qui, C.W. Huang, W.W. Wu, L.

Chang, P.W. Chiu, Y.H. Chu, Oxide heteroepitaxy for flexible optoelectronics, ACS Appl. Mater. Interfaces. 8 (2016) 32401–32407.

[41] C. Li, J. Lin, H. Liu, M. Chu, H. Chen, C. Ma, C. Tsai, H. Huang, H. Lin, H. Liu, Van der Waal epitaxy of flexible and transparent VO_2 film on muscovite, Chem. Mater. 28 (2016) 3914–3919.

[42] C.H. Ma, J.C. Lin, H.J. Liu, T.H. Do, Y.M. Zhu, T.D. Ha, Q. Zhan, J.Y. Juang, Q. He, E. Arenholz, P.W. Chiu, Y.H. Chu, Van der Waals epitaxy of functional MoO_2 film on mica for flexible electronics, Appl. Phys. Lett. 108 (2016) 0–5.

[43] T. Amrillah, Y. Bitla, K. Shin, T. Yang, Y.H. Hsieh, Y.Y. Chiou, H.J. Liu, T.H. Do, D. Su, Y.C. Chen, S.U. Jen, L.Q. Chen, K.H. Kim, J.Y. Juang, Y.H. Chu, Flexible multiferroic bulk heterojunction with Giant magnetoelectric coupling via van der Waals epitaxy, ACS Nano. 11 (2017) 6122–6130.

[44] J. Jiang, Y. Bitla, C.W. Huang, T.H. Do, H.J. Liu, Y.H. Hsieh, C.H. Ma, C.Y. Jang, Y.H. Lai, P.W. Chiu, W.W. Wu, Y.C. Chen, Y.C. Zhou, Y.H. Chu, Flexible ferroelectric element based on van der Waals heteroepitaxy, Sci. Adv. 3 (2017) e1700121.

[45] S. Kim, J.H. Son, S.H. Lee, B.K. You, K. Il Park, H.K. Lee, M. Byun, K.J. Lee, Flexible crossbar-structured resistive memory arrays on plastic substrates via inorganic-based laser lift-off, Adv. Mater. 26 (2014) 7480–7487.

[46] J.Y. Son, Y.H. Shin, H. Kim, H.M. Jang, NiO resistive random access memory nanocapacitor array on graphene, ACS Nano. 4 (2010) 2655–2658.

[47] Z. Sun, L. Wei, C. Feng, P. Miao, M. Guo, H. Yang, J. Li, Built in homojunction dominated intrinsically rectifying resistive switching in NiO nanodots for selection device free memory application, Adv. Electron. Mater. 3 (2017) 1600361.

Table 1 Summary of various transparent flexible memristor devices and memristor composed of NiO layer on rigid substrates

MEMRISTOR MATERIAL	**NIO**	***H*-BN**	**TIO_2/AGNW**	**AL_2O_3**	**ZNO**	**TIO_2**	**NIO**	**NIO**	**NIO**
SUBSTRATE	Mica	PDMS	CPI	PET	PES	PET	Plastic	Nb:STO	Pt/Ti/SiO_2/Si
TRANSFER REQUIRED	No	Yes	No	No	No	No	Yes	No	No
ENDURANCE (#)	1000	500	500	150	200	100	100	200	900
RETENTION(S)	10^5	$5x10^3$	10^5	10^4	10^5	-	10^4	-	-
R_{HLS}/R_{LRS} RATIO	$>10^5$	480	200	$>10^5$	10	>10	30	200	1000
MIN. BENDING RADIUS (MM)	5	14	10	10	20	-	7.5	-	-
BENDING CYCLES@RADIUS	1000@6.5	850@14	No	1000@10	10^4@20	500@-	-	-	-
HIGHEST WORKING TEMPERATURE[^oC]	185	-	-	-	85	-	25	-	-
REFERENCE	This work	[19]	[20]	[28]	[30]	[29]	[45]	[46]	[47]

Figure 1. The photograph and optical properties of ANA/muscovite heterostructure. (a) Flexible and transparent features of the ANA/muscovite heterostructure. Inset shows a schematic of the layer structure. (b) Optical transmittance. (c) XRD 2θ-θ scans of the NiO/AZO/muscovite. (d) ϕ-scans of NiO{022}, AZO{101}, and muscovite{202} diffraction peaks of the ANA/muscovite heterostructure. (e) The cross-sectional TEM images, diffraction patterns, and (f) Schematic illustration of the epitaxial relationship between NiO, AZO, and muscovite layers.

Figure 2. The memristor characteristics of ANA/muscovite heterostructure. (a) I-V curves of five different cells on the ANA/muscovite heterostructure. (b) Electrical endurance and retention performances of the memristor device read at 0.5 V.

Figure 3. The mechanism for the operation of the ANA/muscovite memristor device. (a) Measured and fitted semilogarithmic I-V curves. (b) The plot of logI-logV with the fitted conduction mechanisms in the positive sweep. (c) c-AFM images of the ANA/muscovite memristor device. (d) I-V characteristics at conductive spots in (c). Schematics of the mechanism of the filament in the (e) set and (f) reset processes. Statistical distribution of the size of conductive filaments was showed inset (c).

Figure 4. Temperature-dependent resistive switching behaviors of the ANA/muscovite device. (a) I-V characteristics in the positive voltage at the various operating temperatures from 25 ^{o}C to 185 ^{o}C. (b) The Arrhenius plot. (c) The voltages and (d) the R_{HRS}/R_{LRS} ratio as a function of temperature.

Figure 5. Mechanical flexibility tests of the ANA/muscovite memristor. (a), (b), (c) R_{HRS}/R_{LRS} ratio, endurance, retention with the tensile bending and the compressive bending under various radii. (d), (e), (f) R_{HRS}/R_{LRS} ratio, endurance, retention with the tensile bending and the compressive bending at 6.5 mm of the radius. Images of mechanical flexibility test were observed in inset (a) (tensile) and inset (d) (compressive).

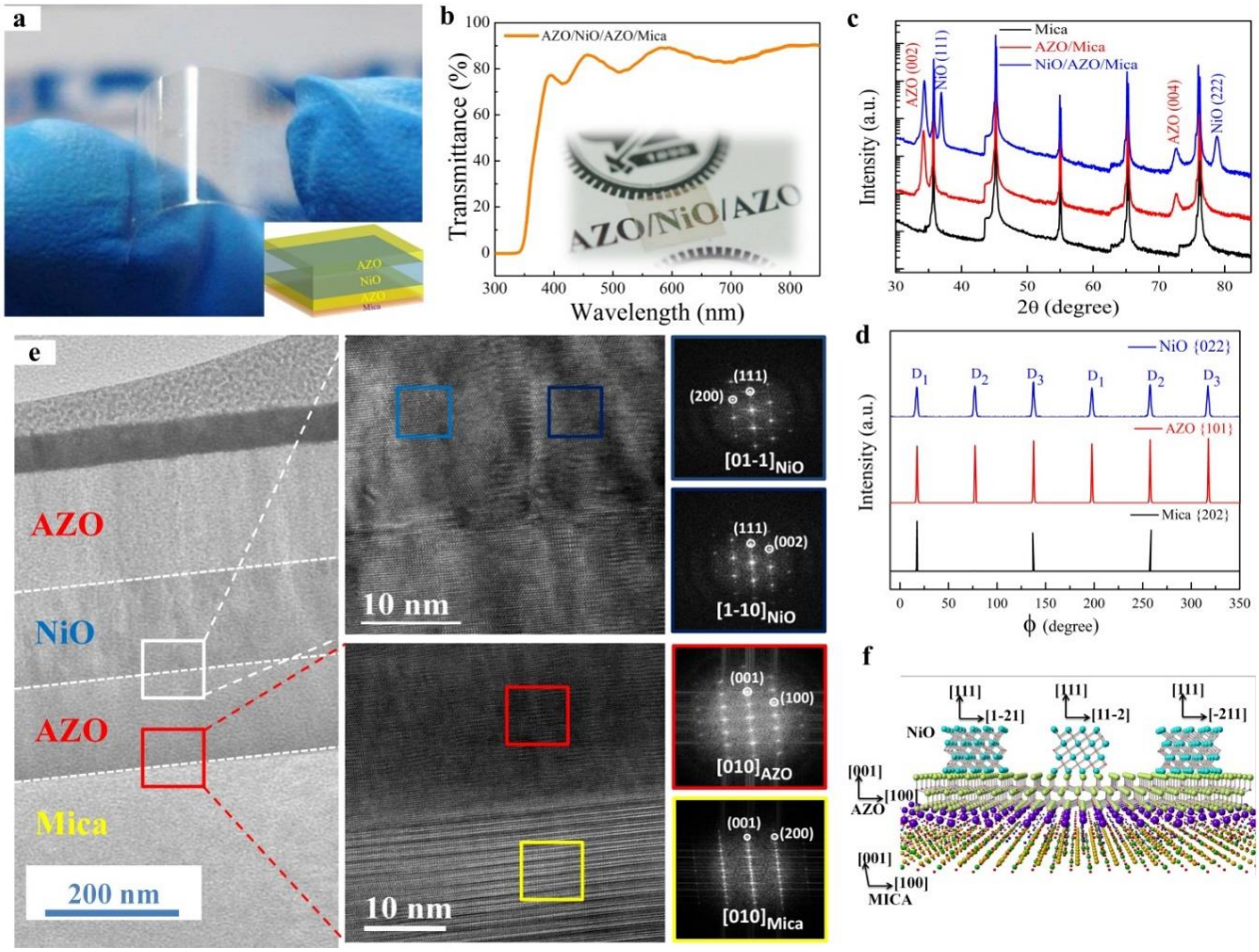
a
AZO
NiO
AZO
Mica
b
AZO/NiO/AZO/Mica
Transmittance (%)
Wavelength (nm)
AZO/NiO/AZO
c
Mica
AZO/Mica
NiO/AZO/Mica
AZO (002)
NiO (111)
AZO (004)
NiO (222)
Intensity (a.u.)
2θ (degree)
d
NiO {022}
AZO {101}
Mica {202}
D1
D2
D3
Intensity (a.u.)
ϕ (degree)
e
AZO
NiO
AZO
Mica
200 nm
10 nm
10 nm
(111)
(200)
[01-1]NiO
(111)
(002)
[1-10]NiO
(001)
(100)
[010]AZO
(001)
(200)
[010]Mica
f
[111]
[1-21]
[111]
[11-2]
[111]
[-211]
NiO
[001]
[100]
AZO
[001]
[100]
MICA

Figure 1

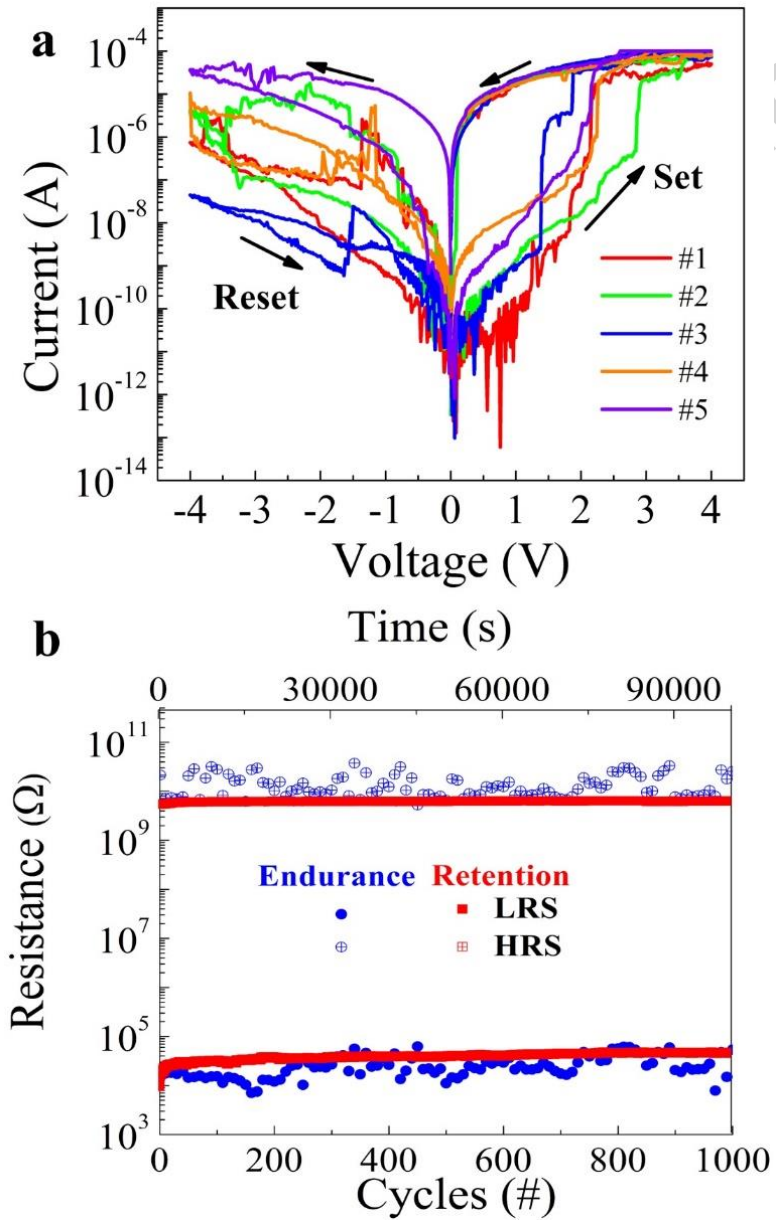
a
Current (A)
Voltage (V)
Set
Reset
#1
#2
#3
#4
#5
b
Time (s)
Resistance (Ω)
Cycles (#)
Endurance
Retention
LRS
HRS

Figure 2

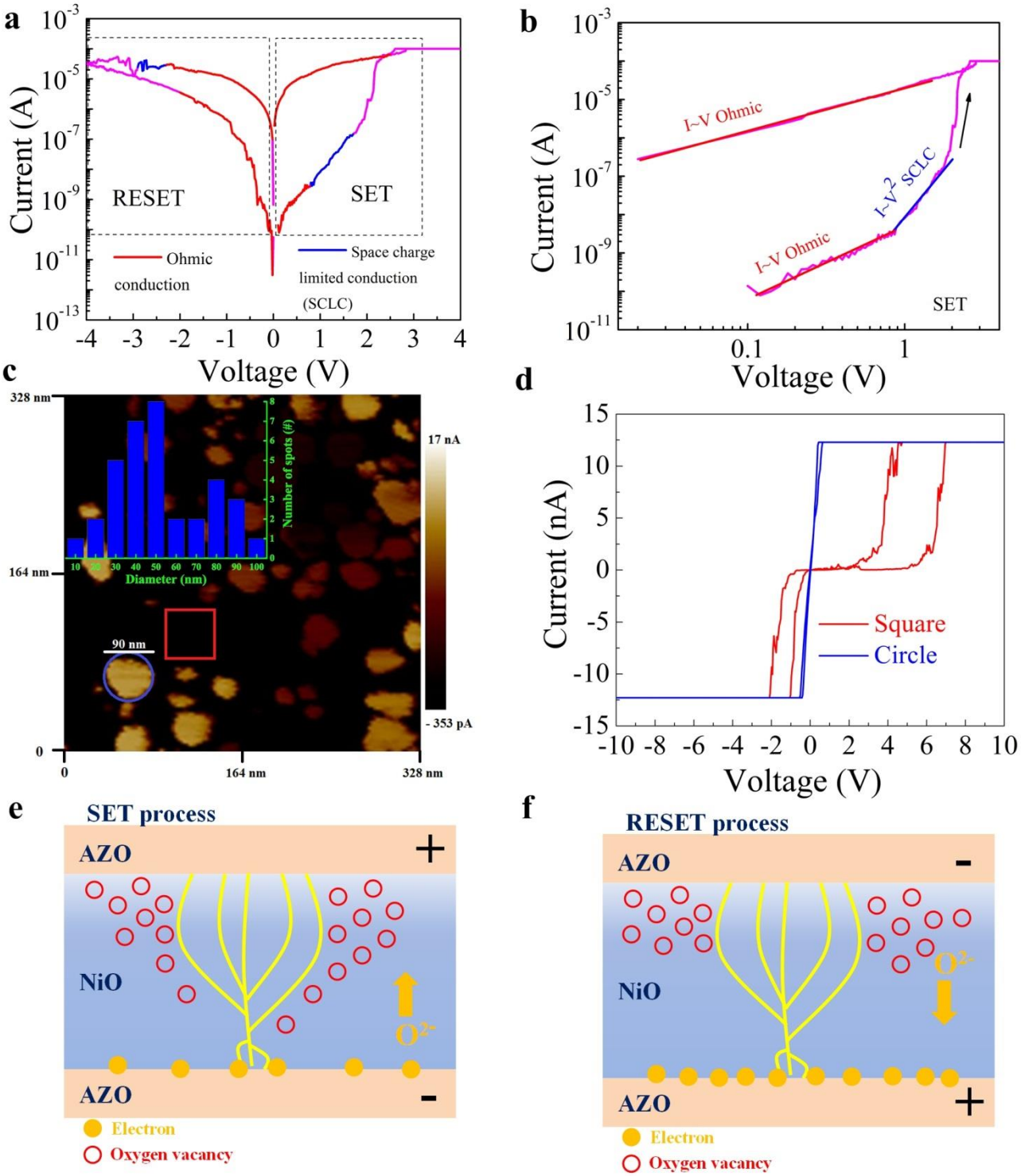

Figure 3

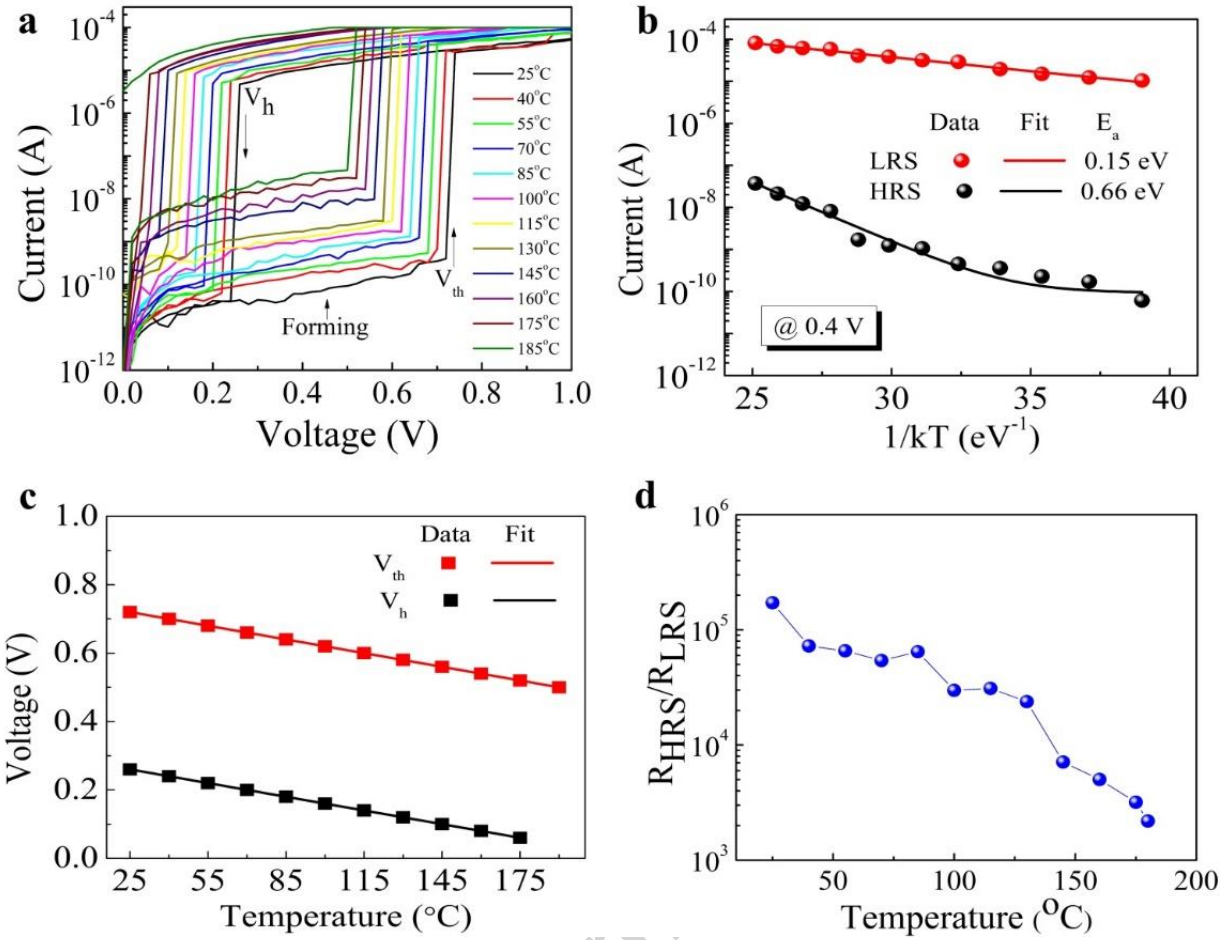

Figure 4

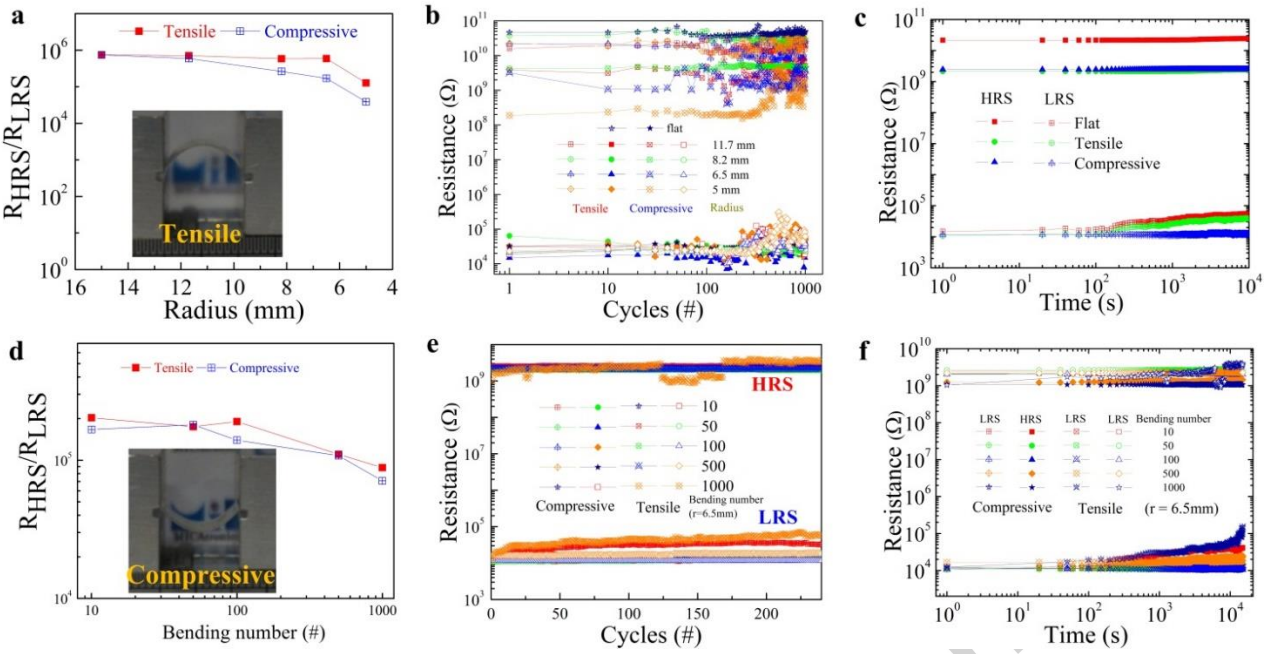

Figure 5

Van-Qui Le

Van-Qui Le is currently a Ph.D. student at Department of Materials Science and Engineering, National Chiao Tung University under the supervision of Prof. Ying-Hao Chu. His current research interest is mainly focused on complex oxides and development of functional nanostructured materials for flexible and transparent oxide electronics.

Thi-Hien Do

Thi-Hien Do received her Ph.D. degree in Materials Science and Engineering from National Chiao Tung University in 2012. She has been serving as a postdoctoral fellow in Institute of Physics, Academia Sinica since 2012. Currently, she is a postdoctoral fellow at Materials Science and Engineering, National Chiao Tung University. Her research expertise is in complex functional oxide heterostructures and nanostructures, transmission electron microscope technique, and X-ray diffraction analysis.

José Ramón Durán Retamal

Dr. José Ramón Durán Retamal received his B.S. (2007) from the Telecommunication Engineering School, Technical University of Madrid, M.S. (2010) from Electrical Engineering Department and Ph.D. (2014) from Graduate Institute of Photonics and Optoelectronics at the National Taiwan University. Currently, he is a postdoctoral fellow at the Computer, Electrical and Mathematical Sciences and Engineering Division of King Abdullah University of Science and Technology

(KAUST). His past research activities include low-dimensional metal oxide structures based electronic nanodevices including transistors, photodetectors, and resistive switching memories. More recently, his research focuses on elucidating and improving the carrier transport through 2D-TMD structures.

Pao-Wen Shao

Pao-Wen Shao received her B.S. degree from Department of Materials Science and Engineering, National Chiao Tung University, Taiwan in 2017. Now she is a Ph. D student at Department of Materials Science and Engineering, National Chiao Tung University.

Yu-Hong Lai

Yu-Hong Lai received his B.S. degree from Department of Materials Science and Engineering, National

Chiao Tung University, Taiwan in 2016. Now he is a Ph. D student at Department of Materials Science and Engineering, National Chiao Tung University.

Wen-Wei Wu

Prof. Wen-Wei Wu received his Ph.D. degree in Materials Science and Engineering from National TsingHua University, 2003. Then he worked as Postdoctoral Fellow (2003–2008) at Materials Science and Engineering, National Tsing Hua University. He joined in Materials Science and

Engineering, National Chiao Tung University from 2008. His main research interests are in situ TEM investigation of dynamical changes in nanostructured materials, synthesis of metal silicide thin films and nanostructures, and metallization on Si and Si–Gealloy.

Jr-Hau He

Dr. Jr-Hau He is an Associate Professor of Electrical Engineering program at King Abdullah University of Science & Technology (KAUST). He has been a pioneer in optoelectronics, which reflects on his achievement of photon management on the light harvesting devices. He has conducted highly interdisciplinary researches to bridge those gaps between various research fields and between academia and industry. He is a Fellow of OSA, RSC and SPIE, and a senior member of IEEE. Visit his web for more information (nanoenergy.kaust.edu.sa).

Yu-Lun Chueh

Yu-Lun Chueh is a professor in Department of Materials Science and Engineering, National Tsing Hua University, Taiwan. His research directions include (1) Direct growth, fundamental characterizations, and optoelectronic applications of two-dimensional materials, including graphene and transition metal dichalcogenide. (2) Energy harvesting by Cu(In,Ga)Se2 solar cells and phase-changed molten salts. (3) Low power resistive random access memory. Details can be found at: http://nanoscienceandnanodevicelab.weebly.com/index.html.

Ying-Hao Chu is an Associate Professor in Department of Materials Science & Engineering, National Chiao Tung University, Taiwan. His research is highly focused on complex functional oxides and strongly correlated electron systems. He has extensive experience in the use of advanced characterization techniques to understand and manipulate functional oxide heterostructures, nanostructures, and interfaces. His current goal is try to create a pathway to use high-quality oxide heteroepitaxy for soft technology. Visit his web for more information: https://sites.google.com/g2.nctu.edu.tw/smartgroup.

Highlights:

Conceptual Insights Statements

- A transparent flexible memristor based on the van der Waals heteroepitaxial grwoth composed of Al-doped ZnO (AZO)/NiO/AZO (ANA) sandwich structure on the muscovite substrate was fabricated.
- ANA/muscovite memristor exhibits not only transparent and flexible memristor with the ON/OFF resistance ratio $>10^5$, the stable endurance to 10^3 cycles and the long retention time of 10^5 s, but also the excellent electrical performances together with the mechanical flexibility, the durability and the thermal stability.
- The ANA/muscovite memristor can work at various bending radii down to 5 mm, the mechanical bending after 1000 cycles at the bending radius of 6.5 mm and the high temperature up to 185 ^oC
- The models of the Ohmic and space-charge-limited conduction (SCLC) and conductive atomic force microscopy (c-AFM) were used to understand the conduction mechanism of the ANA/muscovite memristor during resistive switching.